Eur. Phys. J. C 39, 163–171 (2005)
Digital Object Identifier (DOI) 10.1140/epjc/s2004-02090-1

THE EUROPEAN PHYSICAL JOURNAL C

Inelastic J/ψ and Υ hadroproduction

V.A. Khoze[1,2], A.D. Martin[1], M.G. Ryskin[1,2], W.J. Stirling[1,3]

[1] Department of Physics and Institute for Particle Physics Phenomenology, University of Durham, DH1 3LE, UK
[2] Petersburg Nuclear Physics Institute, Gatchina, St. Petersburg, 188300, Russia
[3] Department of Mathematical Sciences, University of Durham, DH1 3LE, UK

Received: 16 October 2004 / Revised version: 10 November 2004 /
Published online: 11 January 2005 –

Abstract. We consider the prompt hadroproduction of J/ψ, ψ' and the $\Upsilon(1S, 2S, 3S)$ states caused by the fusion of a symmetric colour-octet state, $(gg)_{8s}$, and an additional gluon. The cross sections are calculated in leading-order perturbative QCD. We find a considerable enhancement in comparison with previous perturbative QCD predictions. Indeed, the resulting cross sections are found to be consistent with the values measured at the Tevatron and RHIC, without the need to invoke non-perturbative 'colour-octet' type of contributions.

1 Introduction

It is not easy to describe the hadroproduction of J/ψ mesons within a perturbative QCD framework. The problem is that, due to the $J^P = 1^-$ quantum numbers, it is not possible to directly form the colourless J/ψ meson by gluon-gluon fusion. The simplest possibility is to produce a colour-octet quark-antiquark pair ($gg \to \bar{c}c$) and then to emit an additional gluon, which carries away the colour, as shown in Fig. 1a. This is often referred to as the colour-singlet mechanism (CSM). However the corresponding cross section is suppressed by the small QCD coupling α_s, and by the additional phase space factor associated with the extra gluon emission. As a result the LO QCD prediction [1] is found to be about an order of magnitude lower than the experimental yield of J/ψ mesons.

An alternative and more phenomenological approach is provided by the Colour Evaporation Model (CEM) [2].

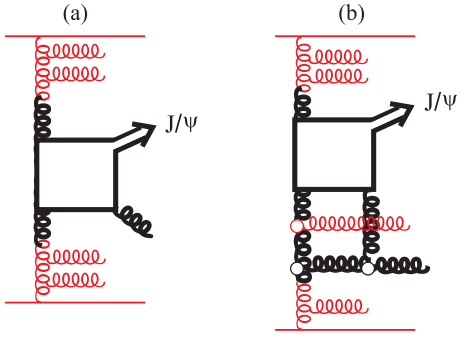

Fig. 1. a The 'bleaching' gluon subprocess used in the original 'colour-singlet' perturbative QCD estimates of prompt J/ψ hadroproduction. **b** The perturbative QCD mechanism studied in this paper. In each case the subprocess $gg \to J/\psi\, g$ is shown in bold

Here the quarkonium production cross section is an (a priori unknown) fraction of the $Q\bar{Q}$ heavy quark cross section integrated over the $m_{Q\bar{Q}}$ invariant mass up to the threshold for producing a pair of the lightest heavy flavour mesons. There are no constraints on the colour or spin of the $Q\bar{Q}$ pair, the transition from colour-octet $Q\bar{Q}$ to colour-singlet quarkonium is assumed to take place by the 'evaporation' of soft gluons. The fraction of $Q\bar{Q}$ pairs that materialise as a particular quarkonium state, $f_{c\bar{c}\to J/\psi}$ for example, is assumed to be universal and is adjusted to give the best fit to existing data.[1] Despite its phenomenological success, the CEM has no firm theoretical foundation. In practice one would not expect the evaporation of soft gluons to take place independently of the particular collision environment, and there is no reason why such soft interactions would not modify the quarkonium production properties, and in particular its collision energy dependence. This is precisely what happens in the theoretically more rigorous formalism for quarkonium production that we introduce below.

The currently most popular and widely used description of quarkonium production is based on a nonrelativistic QCD (NRQCD) effective field theory approach [3], which retains features of both the CSM and CEM. Here $Q\bar{Q}$ pairs are produced via a hard partonic (short-distance) subprocess, in both colour-singlet and colour-octet states, and non-perturbative universal matrix elements describe the (large-distance) transition of the $Q\bar{Q}$ pair into particular quarkonium states.[2]. The cross section of quarkonium H production is written in the schematic form

[1] In practice, it will of course depend on the parameters and pdfs used in the calculation of the $Q\bar{Q}$ cross section.

[2] See, for example, [4–6] and references therein, for a more detailed discussion of the situation, and of the history of the subject.

$$d\sigma(H) = \sum_n d\hat{\sigma}(Q\bar{Q}[n])\ \langle O^H[n]\rangle\,, \qquad (1)$$

where n denotes the set of colour and angular momentum quantum numbers of the $Q\bar{Q}$ pair, and $\hat{\sigma}$ is the cross section of the $Q\bar{Q}$ pair production in a hard subprocess. The non-perturbative transition from the $Q\bar{Q}$ state n into the quarkonium state H is described by a long-distance matrix element $\langle O^H[n]\rangle$. These matrix elements are taken as parameters to be determined by fits to experimental data. In this way, it is possible to compensate the low value of the hard subprocess cross section, $d\hat{\sigma}(Q\bar{Q}[n])$, by the large fitted value of the matrix element $\langle O^H[n]\rangle$. Despite some phenomenological success, a detailed proof of the factorisation formula (1) is lacking, and in particular it is expected to break down at small values of the quarkonium transverse momentum. Predictions for the *total* quarkonium cross section in the NRQCD approach must therefore be treated with caution.

Since the mass of the J/ψ meson is not particularly small, it would be desirable to be able to describe the $Q\bar{Q} \to H$ transition within a perturbative QCD framework. In other words, we would like to consider explicitly an extra gluon exchange (which was *hidden* in the value of the non-perturbative matrix element $\langle O^H[n]\rangle$ in the case of the colour-octet mechanism, i.e., where the J/ψ meson is formed from the colour-octet $Q\bar{Q}$ pair after some non-perturbative interaction described by the $\langle O^H[n]\rangle$ matrix element. The corresponding lowest order in α_s diagrams are shown in Fig. 2. In comparison with the $gg \to Q\bar{Q}$ amplitude, the contributions of Fig. 2 contain an extra loop factor with a small coupling α_s. Here we investigate the possibility that this suppression is compensated by the large number of graphs where the additional (third) gluon, needed to form the J/ψ, is absorbed by different parton-spectators. As viewed from the collinear approximation, the amplitude shown in Fig. 1b, and Fig. 2, corresponds to the next-to-next-to-leading order (NNLO) contribution to the cross section (as compared with LO $gg \to \chi_c$ production). However the second t-channel gluon may be absorbed by *any* parton spectator; that is the amplitude is enhanced by the parton multiplicity, $n \propto \log s$. Therefore it may be considered as the LO amplitude in the BFKL approach. The aim of this paper is to evaluate the numerical size of this enhanced 'NNLO' contribution, and to see if it can remove the large discrepancy between the perturbative QCD prediction and the inelastic J/ψ hadroproduction data.

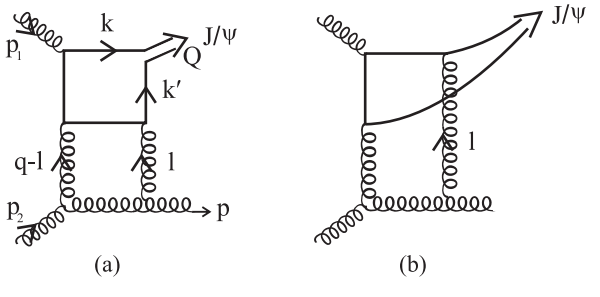

Fig. 2a,b. Lowest-order perturbative QCD diagrams for J/ψ hadroproduction via gluon-gluon fusion with an additional gluon

In Sect. 2 we calculate the amplitude of the process shown in Fig. 2 using the non-relativistic $Q\bar{Q} \to J/\psi$ vertex that was proposed in [7]. Due to the non-relativistic wave function of the J/ψ, there is practically no integration over the quark loop in Figs. 2a,b. Indeed, the J/ψ vertex (i.e., the J/ψ wave function integrated over the relative momenta of the charm quarks), together with the two nearest c-quark propagators is

$$g(\not{k} + m)\gamma_\nu\,, \qquad (2)$$

where the index ν corresponds to the J/ψ polarization vector; and $k_\mu = Q_\mu/2$ and m are the four-momentum and the mass of the c-quark (Q_μ is the momentum of the J/ψ). The constant g may be expressed in terms of the electronic width Γ^J_{ee} of the $J/\psi \to e^+e^-$ decay

$$g^2 = \frac{3\Gamma^J_{ee} M}{64\pi\alpha^2}\,, \qquad (3)$$

where $M = 2m$ is the mass of the J/ψ meson, and the electromagnetic coupling $\alpha = 1/137$.

In Sect. 3 we compute the total cross section of *prompt* inelastic J/ψ hadroproduction at collider energies. That is, in that section, we neglect the additional J/ψ yield coming from b-quark or χ_c decays. We find that the LO result agrees with the Tevatron data rather well. The transverse momentum distributions of prompt J/ψ, ψ' and the $\Upsilon(1S, 2S, 3S)$ production are presented in Sects. 4 and 5, together with a brief discussion of the J/ψ polarization. Alternative possibilities to produce the J/ψ are considered in Sect. 6. One such mechanism is to create a colour-octet $c\bar{c}$ pair, which then transforms to a colour singlet by rescattering via gluon exchange. Another is the associative production of a J/ψ and $c\bar{c}$ pair. The yield from this latter possibility is small. However the first mechanism, where two gluons in a symmetric colour-octet t-channel state, $(gg)_{8s}$, belong to two different Pomerons, may dominate at asymptotically large energies. The energy and rapidity dependence of J/ψ (and Υ) production is given in Sect. 7. Section 8 contains our conclusions.

2 The lowest-order amplitude

We compute the matrix element of the hard subprocess from the diagrams of Fig. 2 in the LO collinear approximation. Thus incoming particles, with momenta p_1 and p_2, are taken to be on-mass-shell, transversely-polarized gluons. The calculation of the amplitude shown in Fig. 2a is similar to the computation of the amplitude for diffractive J/ψ photoproduction [8]. Due to the non-relativistic nature of the J/ψ wave function, the difference between the quark momenta k and k' is very small, that is $|k - k'| \ll m$. Therefore, following [7], we may take $k = k' = Q/2$, and include the integration over the quark loop momentum in the $c\bar{c} \to J/\psi$ coupling g, which is normalized to the width of $J/\psi \to e^+e^-$ decay, see (3).

We expect that the main contribution will come from the region where the rapidity difference between the final gluon

p and J/ψ meson is rather large; that is $s=(p_1+p_2)^2 \gg M^2$. In this limit, the amplitude A^a, corresponding to the diagram Fig. 1a, is

$$\mathrm{Im}\, A^a = \frac{N_c}{8} d^{abc} \int dl_t^2 \; g(4\pi\alpha_s)^{5/2} \tag{4}$$

$$\times \frac{\mathrm{Tr}[\not\varepsilon(\not Q/2+m)\; \not e \not p_2(-\not Q/2-\not l+m)\not p_2(\not Q/2-\not p_1+m)]}{2\pi s[(Q/2-p_1)^2-m^2][l^2-\lambda_g^2][(q+l)^2-\lambda_g^2]} ,$$

where ε and e are respectively the polarization vectors of the J/ψ and the gluon with momentum p_1, and $q=p_1-Q$ is the momentum transferred through the pair of t-channel gluons. $N_c d^{abc}/8$ is the colour factor, where the indices a,b,c are the colours of the two incoming gluons and the final gluon. Bearing in mind possible confinement effects (and to avoid the logarithmic infrared singularity as $q\to 0$) we introduce a cutoff (or effective gluon mass) λ_g in the denominator of (4). Since the two t-channel gluons are in a symmetric colour-octet state, the amplitude A has positive signature. Therefore it has a small real part, $\mathrm{Re}\, A \ll \mathrm{Im}\, A$.

To obtain the whole amplitude, A, we have to add the contribution of the diagram shown in Fig. 2b, which is of the form

$$\mathrm{Im}\, A^b = -\frac{N_c}{8} d^{abc} \int dl_t^2 \; g(4\pi\alpha_s)^{5/2} \tag{5}$$

$$\times \frac{\mathrm{Tr}[\not\varepsilon(\not Q/2-\not l+m)\not p_2(-\not Q/2+m)\; \not e \not p_2(\not Q/2-\not l-\not p_1+m)]}{2\pi s[(Q/2-l-p_1)^2-m^2][l^2-\lambda_g^2][(q+l)^2-\lambda_g^2]} ,$$

where the minus sign reflects the 'negative' colour charge of the antiquark. We also have to account for the contributions where the gluon p_1 couples to the antiquark, and not to the quark. That is, we must include the graphs with the opposite direction of the 'arrows' in the quark loop. Thus the differential cross section is

$$\frac{d\hat\sigma}{dq_t^2} = \frac{|A|^2}{16\pi s^2} , \tag{6}$$

where the total amplitude $A=2(A^a+A^b)$.

For transverse (with respect to the $p_{1\mu}, p_{2\mu}$ plane) J/ψ inelastic production the trace $\mathrm{Tr}[\ldots]=s^2 m(e\cdot\varepsilon)$, while $\mathrm{Tr}[\ldots]=s^2 m(e\cdot Q_t)/M$ when the vector ε corresponds to a longitudinally polarized J/ψ meson. Thus, after averaging over the incoming gluon transverse polarizations, $e^\perp$, the ratio of longitudinal ($\hat\sigma^L$) and transverse ($\hat\sigma^T$) cross sections becomes

$$\frac{d\hat\sigma^L/dq_t^2}{d\hat\sigma^T/dq_t^2} = \frac{|Q_t^2|}{2M^2} . \tag{7}$$

3 The prompt J/ψ yield

In the LO collinear approximation, the cross section of inelastic prompt J/ψ production is of the form

$$\frac{d\sigma}{dy dQ_t^2} = \int \frac{dx_2}{x_2} x_1 g(x_1) x_2 g(x_2) \frac{d\hat\sigma(s,q_t^2)}{dq_t^2} , \tag{8}$$

where y is the centre-of-mass rapidity of the J/ψ meson, $x_1=s/(x_2 S)$, S is the initial hadron-hadron energy squared and $x_i g(x_i)$ are the densities of gluons in the incoming hadrons ($i=1,2$). For a fixed rapidity of the J/ψ meson, the integral over x_2 is equivalent to the integration over the mass $\sqrt{s}$ of the $(J/\psi+g)$ system, where $s=(p_1+p_2)^2$.

The hard subprocess cross section $\hat\sigma$ includes the contribution of the diagrams Fig. 2, where the single gluon p_1 comes from the beam side, plus the 'inverse' contribution, in which the single gluon comes from the target. There is no interference between the original (Fig. 2) and the 'inverse' amplitudes, due to the different colour structure of single and double gluon exchange[3]. Note that single and double gluon exchange correspond, respectively, to antisymmetric and symmetric colour octets.

In the small x region, and at relatively low scales, the gluon distribution behaves like $xg(x)\propto x^{-\lambda}$, where the power $\lambda\sim 0.2$, while the 'hard' subprocess cross section $\hat\sigma$ does not depend on s for $s\gg M^2$. Thus the integral over x_2 takes the form $\int dx_2/x_2^{1+\lambda}$. The main contribution comes from the lowest values of $x_2\simeq M_\perp \mathrm{e}^{-y}/\sqrt{S}$, which correspond to $x_1\simeq M_\perp \mathrm{e}^{y}/\sqrt{S}$, where $M_\perp=(M^2+|Q_t^2|)^{\frac{1}{2}}$. However the essential interval of integration available at collider energies ($\Delta \ln x_2 \approx 1/\lambda \sim 5$) is quite large. This large integration interval partly compensates for the small loop (α_s) factor in the $g(gg)\to J/\psi+g$ amplitude obtained from the diagrams of Fig. 2.

Moreover for an inelastic process we have to allow for the emission of additional (secondary) s-channel gluons from the symmetric octet (gg) (see Fig. 3). This leads to a power growth of the 'hard' subprocess cross section, $\hat\sigma(s)$, as the function of subenergy $\sqrt{s}$. The power behaviour of $\hat\sigma(s)\sim s^\delta$ is driven by the intercept of the amplitude with the four t-channel gluons (the so-called quarteton). Within the leading logarithm approximation ($\sum_n C_n(\alpha_s \ln s)^n$) this intercept was evaluated in [9]. It was shown that numerically the value of δ is, to within 10%, equal to that for the usual BFKL Pomeron (two-gluon) exchange. As a consequence we have to extend the dx_2/x_2 integration over the whole kinematically available rapidity interval Δy. Then the prompt J/ψ cross section becomes

$$\frac{d\sigma}{dy dQ_t^2} = x_1 g(x_1) x_2 g(x_2) \Delta y \frac{d\hat\sigma(s,q_t^2)}{dq_t^2} , \tag{9}$$

with $x_{1,2}=(M_\perp/\sqrt{S})\exp(\pm y)$, and $\Delta y=\ln(x_{\max}^2 S/M_\perp^2)$. We take the same scale, $M_\perp$, for both gluons; different scales are equivalent to a NLO correction to the LO formula. We introduce the factor $x_{\max}=0.3$ to exclude the contribution from the graphs in which the third gluon couples to partons with large $x_{1,2}>0.3$ in the proton fragmentation regions,

[3] The interference would correspond to *odderon*, instead of Pomeron, exchange in the diagram for the cross section. It is known, both experimentally and theoretically, that the odderon-nucleon coupling is small.

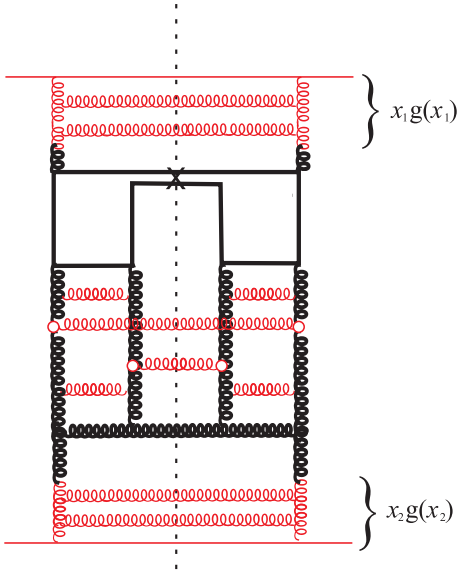

Fig. 3. A contribution to inclusive prompt J/ψ production accompanied by gluon emissions from a t-channel gluon-pair in a colour-symmetric octet. Again, the hard subprocess is shown by bold particle lines

that is to allow for the fact that parton densities at large x are kinematically suppressed.[4]

The formulae in (9) and (6), together with the amplitudes of (4,5), enable the inelastic J/ψ cross section to be predicted. In this way, we find that the cross section at the Tevatron energy $\sqrt{S} = 1.96\,\text{TeV}$ is[5]

$$\sigma(|y| < 0.6) \simeq 2.7\,\mu\text{b} \qquad \text{(pQCD estimate)} \quad (10)$$

in the central rapidity interval $|y| < 0.6$ (integrated over the transverse momentum Q_t). Here we have taken[6] $\lambda_g = 0.8\,\text{GeV}$. This prediction, ((pQCD estimate) (10)), is to be compared with the latest experimental measurement [13]

$$\sigma(|y| < 0.6) = 4.1^{+0.6}_{-0.5}\,\mu\text{b} \qquad \text{(CDF experiment)} \quad (11)$$

The uncertainties of the prediction, (pQCD estimate) (10)) are as follows.

(i) The choice of λ_g. If, instead of 0.8 GeV, we were to take λ_g equal to 0.5 or 1 GeV then $\sigma(|y| < 0.6)$ becomes 4.0 or 2.0 μb respectively.

(ii) The choice of the factorization and renormalization scales. For different scales $\mu = \mu_R = \mu_F$ of $M_\perp/2$, $M_\perp$ and $2M_\perp$, we obtain $\sigma(|y| < 0.6) = 2.7$, 2.3 and 1.5 μb, respectively.

(iii) An unknown K-factor to account for NLO and higher pQCD corrections.

(iv) The uncertainty in the incoming gluon distribution, which is not well constrained at low x and rather low scales.

(v) The choice of the cut-off $x_{\max}$. The variation of the value of $x_{\max}$ plays the role of NLL corrections in the BFKL approach.

Taking all these into account, the expected accuracy of the prediction is about a factor of 2–3 in either direction or even worse.

4 Transverse momentum distribution

Unfortunately we cannot use the amplitudes of (4,5) directly to calculate the Q_t distribution of the produced J/ψ mesons. In the case of diffractive J/ψ photoproduction it is known that the interference between the two lowest-order diagrams, Figs. 2a and b, leads to a dip in the Q_t distribution. Indeed, the differential cross section goes to zero at $Q_t = M$ [14,15]. However this dip disappears after one includes the leading logarithmic ($\alpha_s \ln S$) correction [14,15]. The problem is that we cannot resum the analogous corrections in our case, since the corresponding 'quarteton' eigenfunctions (coming from four gluons in the t-channel) are not yet known.

Therefore, we consider a very simple parametrization

$$d\hat{\sigma}/dQ_t^2 \propto g^2\alpha_s(M_\perp)^5 \log\left(x_{\max}^2 S/M_\perp^2\right)/M_\perp^6 \qquad (12)$$

motivated by dimensional counting, which accounts for the dimension of $g^2 \sim \Gamma M$. Again we take $x_{\max} = 0.3$. The distribution (12) is normalised by equating its Q_t^2 integral to that of (9). In this way the effective gluon mass, λ_g, enters the calculation. The result, shown in Fig. 4, is in reasonable agreement with the Tevatron data [13,16].

In comparison with the colour octet model, where the J/ψ is created in the fragmentation of a gluon jet and the expected distribution is $d\sigma/dQ_t^2 \propto 1/Q_t^4$, in the case of the Fig. 3 subprocess the Q_t distribution (12) at large Q_t is steeper, $d\sigma/dQ_t^2 \propto 1/M_\perp^6$. This is similar to the distribution in the colour-singlet model [1]. However in contrast with the colour-singlet mechanism (Fig. 1a here the hadronic transverse energy flow, which compensates the Q_t of the J/ψ meson, is distributed over a larger rapidity interval in the form of a larger number of gluonic minijets (see Fig. 3).

According to (7) we expect the J/ψ mesons to be transversely polarized at small Q_t, and longitudinally polarized at large Q_t, that is $Q_t \gg M$.[7] At present the data are only

[4] The variation of $x_{\max}$ induces a NLL correction; that is, it is equivalent to an α_s term (without a $\ln(1/x)$ factor) in the BFKL amplitude. Indeed, in the BFKL expansion, the contribution of Fig. 1b to the cross section behaves as an $\alpha_s\Delta y$ term as compared to that of Fig. 1a. Thus the variation of $x_{\max}$ corresponds to an α_s term without a $\ln(S/M^2)$ factor. This does not mean, of course, that the variation of $x_{\max}$ reproduces the *whole* NLL contribution to the BFKL intercept.

[5] We use the LO MRST2001 [10] gluon distribution at scale $\mu = M_\perp/2$, with the corresponding LO (one loop) QCD coupling α_s with $\Lambda^{(4)}_{\text{QCD}} = 220\,\text{MeV}$.

[6] The effective gluon mass λ_g, which occurs in the amplitudes, was first estimated in [11], where it was introduced to describe the photon spectra in $J/\psi \to \gamma gg$ decay. A recent evaluation, together with a collection of previous determinations, is presented in Table 15 of [12]. Based on this Table we choose $\lambda_g = 0.8\,\text{GeV}$, with a possible uncertainty covered by the interval $\lambda_g = 0.5 - 1\,\text{GeV}$.

[7] At next-to-leading order the polarization of the J/ψ may also be affected by the contribution of the longitudinally polarised incoming gluons (p_1 in Fig. 2a), see for example [17].

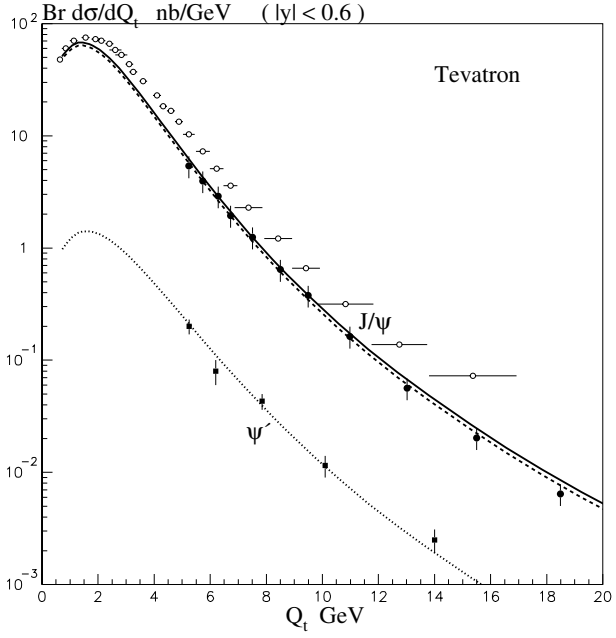

Fig. 4. The transverse momentum (Q_t) distributions of inelastic J/ψ and ψ' production. The data are from [13,16]. The upper and lower data sets for the Q_t distribution of the J/ψ correspond to the total (at $\sqrt{S} = 1.96\,\text{TeV}$) and prompt (at $\sqrt{S} = 1.8\,\text{TeV}$) J/ψ yields respectively; recall that our QCD prediction is for prompt production only

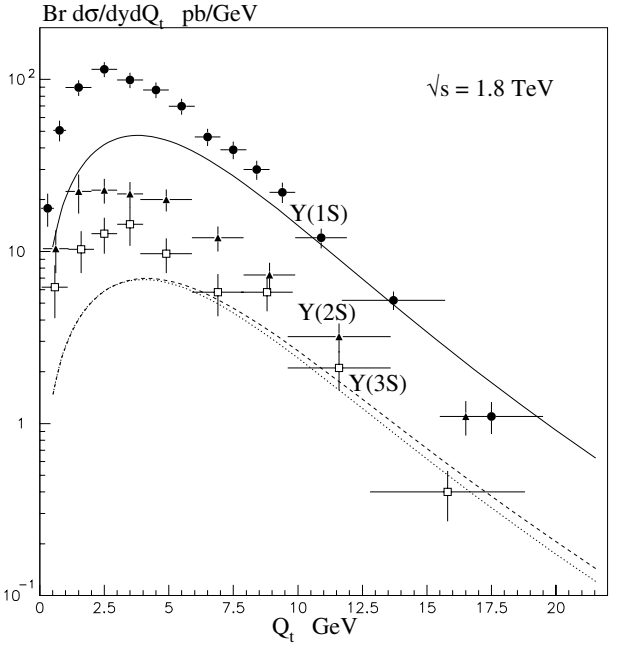

Fig. 5. The Q_t distributions of the inelastic production of the Υ states, compared with Tevatron data [20]

available in the interval of $Q_t \sim 4 - 20\,\text{GeV}$, where the observed J/ψ is approximately unpolarized. The parameter $\alpha < 0.3$ of [18] corresponds to a small transverse polarization at lower Q_t values. However, as Q_t increases α changes sign and for $Q_t > 15\,\text{GeV}$ clearly indicates longitudinal polarization of the J/ψ. This is qualitatively consistent with our expectations. In contrast, colour-octet models of prompt J/ψ production lead to transverse polarization at large Q_t [19].

5 Prompt $\psi'(2S)$ and Υ production

The above formalism can be applied to the production of other quarkonium states by simply changing the mass and width of the $J^P = 1^-$ heavy $Q\bar{Q}$ resonance. Thus, without any free parameters, we can predict the cross section for inclusive prompt quarkonium production. The results for ψ' and for the upsilon states are compared with the Tevatron data [16, 20] in Fig. 4 and Fig. 5 respectively. We use the effective gluon mass λ_g and the scale that were appropriate for the description of the J/ψ data. In this way we remove a large part of the uncertainty in the prediction for ψ'. The good agreement with the ψ' data should therefore be regarded as support for our perturbative QCD approach.

The comparison of the prompt Υ predictions with the Tevatron data, shown in Fig. 5, is complicated, however, since only half of the total $\Upsilon(1S)$ yield arises from prompt production [21]. Moreover, the χ_b states have a large branching fraction of radiative decays to $\Upsilon(2S)$; about twice as large as those to $\Upsilon(1S)$. Bearing in mind these complications, and the uncertainties in the predictions, the agreement with the data is better than may have been expected.

The predicted cross sections for prompt J/ψ, ψ'; $\Upsilon(1S, 2S, 3S)$ central production at the Tevatron energy, $\sqrt{S} = 1.96\,\text{TeV}$, are

$$d\sigma/dy|_{y=0} = 2.2,\ 0.6\,\mu\text{b};\quad 40,\ 12,\ 9\,\text{nb}\,,\ \text{(Tevatron)} \quad (13)$$

respectively; and correspondingly at the LHC energy, $\sqrt{S} = 14\,\text{TeV}$,

$$d\sigma/dy|_{y=0} = 8.1,\ 2.5\,\mu\text{b};\quad 310,\ 100,\ 80\,\text{nb}\,.\ \text{(LHC)} \quad (14)$$

6 Other production mechanisms

6.1 Uncorrelated gluon-gluon pairs

Besides the diagrams shown in Fig. 3, where two t-channel gluons in a symmetric colour octet state are placed rather close to each other in the impact parameter (b_t) plane, there may also be a contribution from diagrams like those shown in Fig. 6. This may be viewed as the production of a colour-octet $c\bar{c}$ pair that subsequently changes colour via rescattering. Here the two t-channel gluons in the amplitude belong to two different Pomerons, that is to two different parton showers. A convenient way to calculate such a contribution is to use the AGK cutting rules [22], that is to calculate diagram Fig. 6b and then use the relation

$$\sigma^{\text{Fig. 6a}} = 2\sigma^{\text{Fig. 6b}}\,. \quad (15)$$

Strictly speaking, the two gluons in the lower (left or right) parts of Fig. 6b cannot form a colour-singlet (Pomeron)

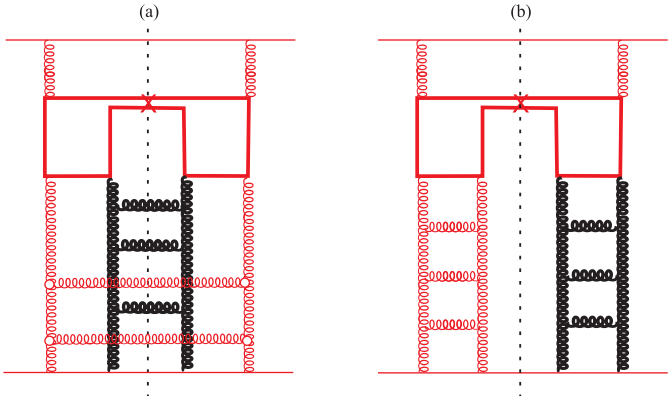

Fig. 6. Prompt J/ψ **a** inelastic and **b** single diffractive production arising from an interaction in which the two t-channel gluons belong to different Pomerons. One Pomeron is shown in bold, the other in fainter print

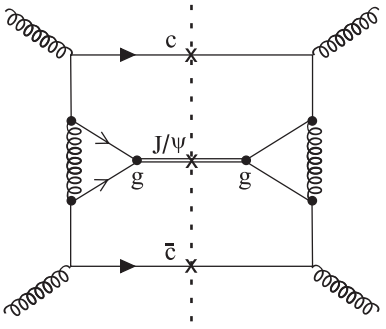

Fig. 7. The diagram used to compute the associated production of J/ψ together with a $c\bar{c}$ pair. The t-channel gluon is needed in order to put the virtual t-channel charm quarks on mass shell

state. On the other hand, these two gluons are in a colour *symmetric* state, and therefore we may use the AGK relation (15) to simplify the calculation.

The amplitude corresponding to Fig. 6b is very similar to that of Fig. 3. The main difference is that now the density of the second t-channel gluon is given by an independent gluon distribution $xg(x)$. That is, we need the probability to find two gluons $w_{gg} \approx (xg(x))^2$. On the other hand these two gluons are uniformly distributed over the whole transverse area occupied by a proton. Therefore the integration over the transverse momentum Q_t is limited by the 'elastic' slope B, which may be taken from the slope observed for diffractive J/ψ photoproduction; that is $B \sim 4.5\,\mathrm{GeV}^{-2}$ [23]. Thus we can consider the lowest-order amplitudes given by (4,5) at $Q_t = 0$, and take the integral $\int dQ_t^2 = 1/B$.

The factor $(N_c\alpha_s/\pi)^2$, together with two logarithmic integrations, dl_t^2/l_t^2, in each amplitude[8], becomes the gluon distribution $w_{gg} = (xg(x))^2$ in the cross section. Next we have to account for an extra $1/2$ in the colour factor, which is cancelled by the factor 2 in the AGK relation (15). Thus, finally, we obtain

$$\frac{d\sigma^{\text{Fig. 6a}}}{dy} = \frac{10\pi^4\alpha_s^3 g^2}{3BM^6} x_1g(x_1)x_2g(x_2)[x_1g(x_1) + x_2g(x_2)]\,. \tag{16}$$

Using MRST2001 LO gluons [10], we find that[9] $\sigma^{\text{Fig.6}a}(|y| < 0.6) = 2.2\,\mu$b, at the Tevatron energy $\sqrt{S} = 1.96$ TeV. This is smaller than the main contribution discussed in Sect. 3. However at larger energies the 'two Pomeron' cross section will grow faster than the contribution of Sect. 3. Indeed

$$\sigma^{\text{Fig. 6a}} \propto x_1g(x_1)(x_2g(x_2))^2 \propto x_1^{-\lambda}x_2^{-2\lambda} \propto S^{3\lambda/2} \tag{17}$$

in the central region of small y, where $x_i \propto 1/\sqrt{S}$, whereas the cross section (9) is proportional to $S^\lambda \ln S$ only. In particular, at the LHC energy $\sqrt{S} = 14$ TeV we expect in the centre of the rapidity plateau $d\sigma^{\text{Fig.6}a}(y=0)/dy = 6.7\ \mu$b, while the cross section (9) is $d\sigma^{\text{Fig.3}}(y=0)/dy = 8.1\ \mu$b.

At first sight, the transverse momentum distribution of the J/ψ for the contributions of Fig. 6 should be peaked at low Q_t, namely $Q_t^2 \sim 1/B$. This is true for the contribution of the diagram Fig. 6b, but not for the inelastic process, Fig. 6a. The emission of intermediate gluons spreads out the J/ψ distribution from the inelastic process, so that we expect a spectra

$$d\hat{\sigma}^{\text{Fig.6}a}/dQ_t^2 \propto g^2\alpha_s(M_\perp)^3/M_\perp^6\,, \tag{18}$$

analogous to (12).

We must of course take care of possible double counting. Note that the amplitudes shown in Fig. 6a and Fig. 3 are very similar, and the gluon densities given by the global parton analyses do not distinguish the gluons coming from one or more parton showers. Therefore, to be conservative, in what follows we consider only the contribution of Fig. 3. A possible contribution of Fig. 6a is well within the uncertainties of the lowest-order in α_s calculations.

6.2 Associative ($J/\psi + c\bar{c}$) production

Another possibility is to consider the production of a J/ψ meson together with a $c\bar{c}$ pair, as shown in Fig. 7. In this case the expected hard cross section at the Tevatron is about $\hat{\sigma}(c\psi\bar{c}) \sim 2$ nb, leading to

$$\left.\frac{d\sigma(c\psi\bar{c})}{dy}\right|_{y=0} = \hat{\sigma}\ x_1g(x_1)\ x_2g(x_2) \ \sim\ 0.05\ \mu\text{b}\,. \tag{19}$$

For inelastic hadroproduction, the contribution coming from this mechanism is not large, of the order of 1% . However in e^+e^- annihilation, associative production is much more important, see for example [24]. Indeed, in e^+e^- annihilation there is no suppression for the production of the first $c\bar{c}$-pair. On the other hand for time-like annihilation kinematics the third t-channel gluon (l in Fig. 2) can couple to the nearest parton only[10]. Thus we loose the

[8] The lowest-order gluon distribution at low x is given by the first iteration of the DGLAP equation, that is $xg(x) = (N_c\alpha_s/\pi)\int dl^2/l^2$

[9] We take the scale $\mu = M/2$ both in the gluon distribution and in the QCD coupling α_s.

[10] Otherwise we destroy the leading logarithms.

enhancement caused by a large parton multiplicity, that is the factor $\Delta y \sim \ln(S/M^2)$ in (9). Without this factor the contributions of single (Fig. 2) and associative (Fig. 7) production are expected to be of the same order (in agreement with the measurements of the Belle collaboration for e^+e^- annihilation [25]).

Note that if the inelastic J/ψ hadroproduction were to originate from 'colour-octet' dynamics, that is the main yield of J/ψ were to come from gluon $g^* \to J/\psi + \ldots$ fragmentation [3,26], then we would expect the same ratio of 'direct' to 'associative' contributions in e^+e^- annihilation, as that for hadroproduction, contrary to our perturbative QCD predictions.

6.3 Production via χ_c and $b\bar{b}$ decays

Finally we have the possibility of non-prompt J/ψ production. Experimentally it is observed that a fraction of J/ψ mesons originate from $\chi \to J/\psi + \gamma$ and $b \to J/\psi + X$ decays. We do not discuss here the details of these production mechanisms. However in order to predict the *total* J/ψ yield we estimate these contributions using the experimental data of [27,28] and collinear factorization. Symbolically, the relation that we use is of the form[11]

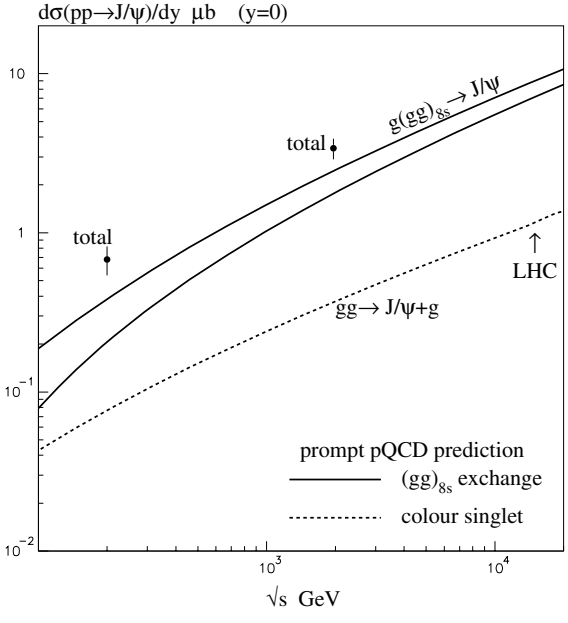

Fig. 8. The energy dependence of *prompt* J/ψ production obtained from the colour-singlet mechanism, $gg \to J/\psi\ g$, is shown by the dashed curve. The contribution obtained from our subprocess, $g(gg)_{8s} \to J/\psi$, is shown by continuous curves with $x_{\max} = 0.1$ (lower) and 0.5 (upper). Also shown are the values for the *total* J/ψ yield measured at RHIC [29] and the Tevatron [13]

[11] The relation also happens to hold for χ_1 production, despite the fact that it cannot be formed by gluon-gluon fusion. The dominant mechanism for χ_1 production is the process with antisymmetric colour-octet gg exchange. However, since this exchange corresponds to gluon Reggeization, it has the same energy (and x) dependence as the exchange of a single gluon.

$$d\sigma/dy = x_1 g(x_1)\ \hat{\sigma}\ x_2 g(x_2)\,, \qquad (20)$$

where $y = \frac{1}{2}\ln(x_1/x_2)$ and the normalisation of $\hat{\sigma}$ is adjusted to fit the χ and $b\bar{b}$ data. Since the energy dependence of the cross section is driven simply by the x dependence of the gluon densities, the experimental data at one fixed energy are sufficient to estimate these non-prompt contributions at other energies[12].

7 Energy and rapidity dependence

In comparison with the usual perturbative QCD colour-singlet (Fig. 1a) and colour-evaporation mechanisms, where the energy dependence is essentially determined by the product of the gluon densities, see (20), our perturbative contribution to the cross section (Fig. 1b is enhanced by an additional $\log S$ factor, Δy in (9). Therefore the energy dependence of these two contributions is different, as can be seen in Fig. 8. To demonstrate the uncertainty arising from the choice of the cut-off $x_{\max}$ in the additional logarithm Δy in the computation of the new perturbative contribution, we show predictions for the two values, $x_{\max} = 0.1$ (lower curve) and 0.5 (upper curve).

Note that the amplitude of the new subprocess is calculated at lowest order in α_s. It is not unusual to have a next-to-leading order K factor of the order of two for the production of relatively low-mass states, as in Drell-Yan production for example. On the other hand, we see no reason for a strong energy dependence of such a K factor. So, noting the good agreement with the Tevatron data, we expect our predictions at the LHC energy to be reliable.

The energy behaviour of the total inelastic J/ψ cross section in the fixed-target/ISR to Tevatron energy interval is shown in Fig. 9, together with the components from the following subprocesses: $g(gg)_{8s} \to J/\psi$, $gg \to J/\psi\ g$, $\chi_c \to J/\psi$ and $b\bar{b} \to J/\psi$. We see that the cross section is slightly underestimated at the lower energies, where a contribution initiated by the $q\bar{q}$ subprocess, that is by secondary Reggeons, may have some influence. Indeed, it was noted in [31] that the difference between the J/ψ production cross sections from pp and $p\bar{p}$ interactions indicates a noticeable $q\bar{q}$ contribution at the lower energies.

In Fig. 10 we show predictions for the rapidity distributions of J/ψ and $\Upsilon(1S)$ production at both the Tevatron (1.96 TeV) and LHC[13] (14 TeV) energies. In Table 1 we compare our results for the total J/ψ and $\Upsilon(1S)$ cross

[12] In [27] the cross section was given for χ production in the forward hemisphere. Therefore to normalize the J/ψ cross section, we use (20) to calculate the integrated cross section.

[13] Note that the General Purpose Detectors ATLAS and CMS can only measure the high transverse momentum tail of quarkonium production, the majority of the final-state leptons falling below the trigger thresholds. The ALICE detector, on the other hand, is ideally suited to a measurement of both charm and bottom quarkonium cross sections [6,32]. ALICE can measure electrons and muons down to very low transverse momentum ($\mathcal{O}(1\ \mathrm{GeV}/c)$) in the pseudorapidity ranges $|\eta_e| < 0.9$ and $2.5 < |\eta_\mu| < 4.0$, respectively. This gives non-zero acceptance for the J/ψ down to $p_T(J/\psi) = 0$, see Figs. 60 and 63 of [6].

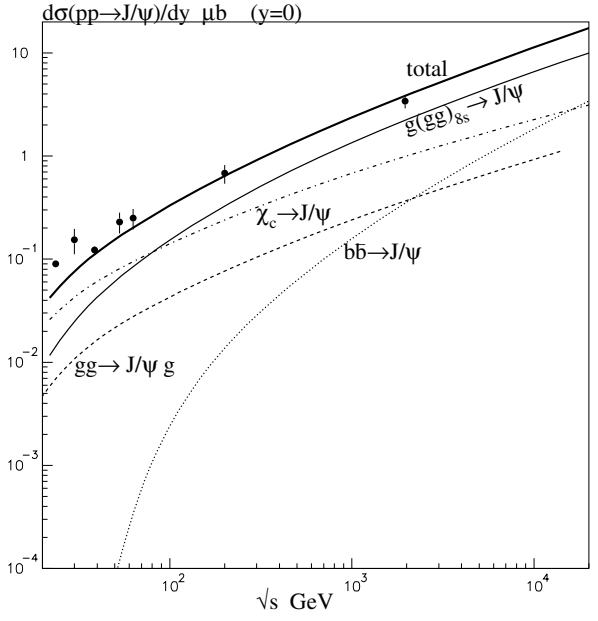

Fig. 9. The energy dependence of inelastic J/ψ production compared with a selection of the available data from fixed-target pN to Tevatron $p\bar{p}$ collider energies [13,29,30]. Besides the total (bold curve), we also display the prompt ($g(gg)_{8s} \to J/\psi$ and $gg \to J/\psi\ g$) and non-prompt ($\chi_c \to J/\psi$ and $b\bar{b} \to J/\psi$) components

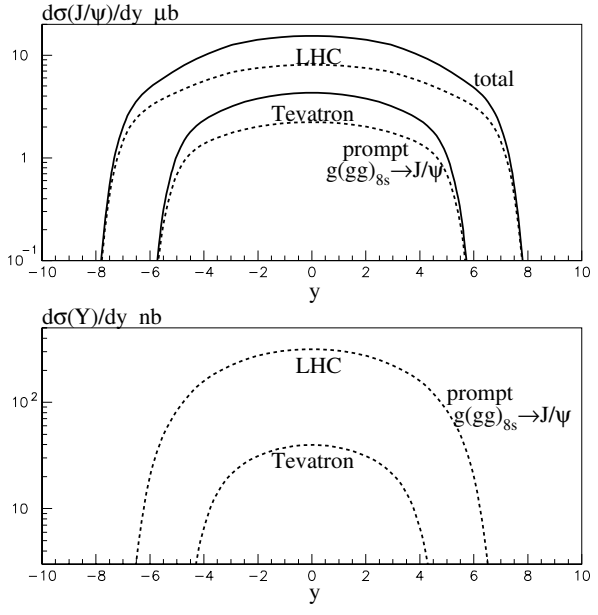

Fig. 10. The rapidity distributions of J/ψ and $\Upsilon(1S)$ production at Tevatron and LHC energies. The continuous and dashed curves correspond to the total and prompt yields respectively

sections at LHC with the predictions of the CEM (taken from [6]). Note that our predicted cross sections are systematically larger because of the steeper $\sqrt{S}$ dependence caused by the $\log(S/M_\perp^2)$ factor in (9).

Table 1. The predictions for J/ψ and $\Upsilon(1S)$ cross sections (in μb) at the LHC. For the J/ψ, the 'total' cross section includes the additional contributions from χ_c and $b\bar{b}$ decay. The CEM predictions are taken from Tables 9 and 10 in [6]

		pQCD	CEM
$\sigma_{J/\psi}$(prompt)	(μb)	80	33
$\sigma_{J/\psi}$(total)	(μb)	150	54
$\sigma_{\Upsilon(1S)}$(prompt)	(μb)	2.5	0.4

8 Conclusions

We have calculated the prompt hadroproduction of J/ψ, ψ' and $\Upsilon(1S, 2S, 3S)$ states within a perturbative QCD framework, without any non-perturbative contributions (such as occur explicitly in the NRQCD colour-octet model and implicitly in the CEM). Recall that the original colour-singlet LO perturbative contribution (based on the subprocess $gg \to J/\psi\ g$) falls well short of the data. However, here, we have studied another perturbative QCD contribution, which turns out to be dominant. The basic subprocess is $g(gg)_{8s} \to J/\psi$, see Figs. 2,3 or Fig. 1b. This contribution is enhanced, particularly at high energies, since the additional t-channel gluon can couple to a large number of parton spectators.

The uncertainties of such a computation are listed at the end of Sect. 3. They are not small. However, with our natural choices of scale and of the effective gluon mass, we successfully describe the available high-energy RHIC and Tevatron J/ψ data. In addition, without any new parameters, we obtain an excellent description of the ψ' data, and even a satisfactory description of Υ production.

There is additional qualitative support for the $g(gg)_{8s} \to J/\psi$ mechanism coming from the measurement of the J/ψ polarization at the Tevatron. This mechanism predicts a longitudinal polarization at large Q_t, in agreement with the data, whereas the colour-octet model leads to a transverse polarization [19].

Acknowledgements. We thank Anatoli Likhoded, Lev Lipatov and Orlando Villalobos-Baillie for useful discussions. ADM thanks the Leverhulme Trust for an Emeritus Fellowship and MGR thanks the IPPP at the University of Durham for hospitality. This work was supported by the UK Particle Physics and Astronomy Research Council, by a Royal Society special project grant with the FSU, by grant RFBR 04-02-16073 and by the Federal Program of the Russian Ministry of Industry, Science and Technology SS-1124.2003.2.

References

1. R. Baier, R. Ruckl, Phys. Lett. B **102**, 364 (1981); Z. Phys. C **19**, 251 (1983)
2. V.D. Barger, W.Y. Keung, R.J.N. Phillips, Phys. Lett. B **91**, 253 (1980); Z. Phys. C **6**, 169 (1980)
3. G.T. Bodwin, E. Braaten, G.P. Lepage, Phys. Rev. D **46**, 1914 (1992); Phys. Rev. D **51**, 1125 (1995); Erratum Phys. Rev. D **55**, 5853 (1997); E. Braaten, S. Fleming, Phys. Rev. Lett. **74**, 3327 (1995)

4. E. Braaten, S. Fleming, T.C. Yuan, Ann. Rev. Nucl. Part. Sci. **46**, 197 (1996); M. Beneke, [arXiv:hep-ph/9703479]
5. Cong-Feng Qiao, J. Phys. G **29**, 1075 (2003), [arXiv:hep-ph/0202227]
6. R. Vogt, S. Frixione et al., [arXiv:hep-ph/0311048]
7. E.L. Berger, D. Jones, Phys. Rev. D **23**, 1521 (1981)
8. M.G. Ryskin, Z. Phys. C **57**, 89 (1993)
9. L.N. Lipatov, H. de Vega, Phys. Rev. D **66**, 074013 (2002)
10. A.D. Martin, R.G. Roberts, W.J. Stirling, R.S. Thorne, Phys. Lett. B **531**, 216 (2002)
11. G. Parisi, R. Petronzio, Phys. Lett. B **94**, 51 (1980)
12. J.H. Field, Phys. Rev. D **66**, 013013 (2002)
13. CDF Collaboration, Tara Shears, Fermilab-CONF-03/350-E, Oct. 2003
14. J.R. Forshaw, M.G. Ryskin, Z. Phys. C **68**, 137 (1995)
15. J. Bartels, J.R. Forshaw, H. Lotter, M. Wüstoff, Phys. Lett. B **375**, 301 (1996)
16. CDF Collaboration, F. Abe et al., Phys. Rev. Lett. **79**, 572 (1997)
17. N.N. Nikolaev, Nucl. Phys. A **699**, 210 (2002)
18. CDF Collaboration, T. Affolder et al., Phys. Rev. Lett. **85**, 2886 (2000)
19. P. Cho, M. Wise, Phys. Lett. B **346**, 129 (1995); M. Beneke, M. Kramer, Phys. Rev. D **55**, 5269 (1997); E. Braaten, B. Kniehl, J. Lee, Phys. Rev. D **62**, 094005 (2000)
20. CDF Collaboration, D. Acosta et al., Phys. Rev. Lett. **88**, 161802 (2002)
21. CDF Collaboration, T. Affolder et al., Phys. Rev. Lett. **84**, 2094 (2000)
22. V.A. Abramovsky, V.N. Gribov, O.V. Kancheli, Sov. J. Nucl. Phys. **18**, 308 (1974)
23. H1 Collaboration, S. Aid et al., Nucl. Phys. B **472**, 3 (1996); C. Adloff et al., Eur. Phys. J. C **10**, 373 (1999); Phys. Lett. B **483**, 23 (2000); ZEUS Collaboration, J. Breitweg et al., Z.Phys. C **75**, 215 (1997); Eur. Phys. J. C **6**, 603 (1999)
24. A.B. Kaidalov, JETP Lett. **77**, 349 (2003); B.L. Ioffe, D.E. Kharzeev, Phys. Rev. D **69**, 014016 (2004)
25. Belle Collaboration, K. Abe et al., Phys. Rev. Lett. **89**, 142001 (2002)
26. V.A. Saleev, D.V. Vasin, Phys. Rev. D **68**, 114013 (2003)
27. E771 Collaboration, T. Alexopoulos et al., Phys. Rev. D **62**, 032006 (2000)
28. CDF, D0 Collaborations, Chunhui Chen, [arXiv:hep-ex/0401021]
29. R.G. de Cassagnac, [arXiv:nucl-ex/0403030]
30. C. Kourkoumelis et al., Phys. Lett. B **91**, 481 (1980); L. Antoniazzi et al., Phys. Rev. D **46**, 4828 (1992); T. Alexopoulos et al., Phys. Rev. D **55**, 3927 (1997)
31. A.D. Martin, R.G. Roberts, W.J. Stirling, Phys. Rev. D **37**, 1161 (1988)
32. ALICE collaboration, Physics Performance Report, Vol. 1, CERN/LHCC 2003-049 (2003), to be published in J. Phys. G